TELKOMNIKA, Vol.17, No.6, December 2019, pp.2877~2884
ISSN: 1693-6930, accredited First Grade by Kemenristekdikti, Decree No: 21/E/KPT/2018
DOI: 10.12928/TELKOMNIKA.v17i6.13004

Study the effect of thin film thickness on the optical features of (IR5 laser dye/CdSe nanoparticles) samples

Mithaq M. Mehdy Al- Sultani*
Department of Physics, College of Education for Girls, Kufa University, Iraq
*Corresponding author, e-mail: mithaqmehdyal_sultani@yahoo.com

Abstract

The linear optical features such as (transmittance T, absorbance A, the effective length L_{eff}, absorption coefficient α and refractive index n) for the thin films samples of (3x10^{-3} mol/l of (IR5) laser dye, 0.02 gm of (CdS) nanoparticles and 0.04 gm of pp polymer) had been studied at different values of film thickness in one time and at different number of Yb:GdVO$_4$ laser pulses. The non-linear optical features in terms of transmittance difference ΔT_{p-v}, non-linear refractive index n_2, non–linear phase shift $\Delta\Phi_o$ non-linear absorption coefficient β and minimum normalized transmittance $T(Z)$ have been computed in relation to obtained normalized transmittance data from setup of Z-scan with open and closed apertures, calculated for (3x10^{-3} mol/l of (IR5) laser dye, 0.02 gm of (CdSe) nanoparticles and 0.04 gm of (pp) polymer) thin films at different values of film thickness at in one time and at different Yb:GdVO$_4$ laser pulses. Thick films causes in deleting the non-linear effects generated by different layers. The (CdSe) nanoparticles leads to an absorption shifting of the wavelengths to lengthier wavelengths of red shift. So, this can be used in selecting the nanoparticles and medium with applicable exciting wavelengths. The film thickness and the laser pulses have the main effects in consolidating the Non-linear optical features.

Keywords*: CdSe nanoparticles, IR5 laser dye, non-linear optical features, thickness*

1. Introduction

IR 5 laser dye is of ($C_{50}H_{43}O_6Cl$) chemical composition and it has (775.34) molecular weight. It has dark green colour. This dye appears as a crystalline solid, but it can be dissolved in dichloroethane organic polar solvent. It has maximum absorption at (1090 nm) and (9.30x10^4 mol^{-1}.cm^{-1}) molar absorptivity [1]. In 1981, R.R. Alfano et al., presented a study for using IR 5 as a laser medium for dye laser pumped by Nd: YAG laser, where it had the peak laser wavelength at (1320 nm) and coverage range about (1180–1400) nm [2]. CdSe nanoparticles are of ($\sim 5\ nm$) exciton radius, ($1.74\ eV$) band gap energy. It has the fluorescence emission at ($570\ nm$) with fluorescence intensity of ($2.1\ a.u$) [3].In 1998, E. Lifshitz et al., prepared the CdSe nanoparticles by the two different methods as (chemical solution deposition and development in a silica sol–gel matrix) and showed essentially the same optical behavior [3]. In 2004, S. Zhang et al., studied the photoluminescence features of mercaptocarboxylic acid-stabilized CdSe nanoparticles adjusted by coating with polyelectrolyte. The negative charged polyelectrolyte PSS has no influence on the trap and intrinsic emitting of CdSe nanoparticles [4]. In the same year, I. Sondi et al., prepared at room temperature Water-Dispersible Amdex-CdSe nanoparticle complexes by speedily combination of aqueous solutions of either sodium selenide with those of cadmium chloride. It had been concluded that CdSe crystallite size in the precipitation process has reduced with increased polymer content [5].

In 2009, P. Gupta and M. Ramrakhiani, presented an investigation about the effect for the particle size in the optical features of CdSe nanoparticles [6, 7]. Polypropylene (PP) polymer, also so-called polypropene, stands for a thermoplastic polymer employed in various uses. It can be manufactured from the monomer propylene by chain-growth of polymerization. It has the chemical formula of $(C_3H_6)_n$ and 0.946 g/cm^3 density and 403 to 444 K melting point. It can be used in different fields as industry, medical, clothing, recycling and repairing [8-12]. In this research, as compared with [2-12]**,** we will study specifically the linear optical features such as (transmittance T, absorbance A, the effective length L_{eff}, absorption coefficient α and refractive index n) for the thin films samples of (3x10^{-3} mol/l of (IR5) laser dye, 0.02 gm of

Received April 27, 2019; Revised July 2, 2019; Accepted July 18, 2019

(CdSe) nanoparticles and 0.04 gm of pp polymer) at different values of film thickness in one time and at different number of Yb:$GdVO_4$ laser pulses.

2. Research Method

2.1. Absorption Spectral Features

The process of absorption is feasibly taken place in the case of the corresponding photon crashes the dye molecule in its minor energy state. The dye is feasibly motivated as a result of absorbed photon and its employed energy in the excitation of dye. The absorption takes place at them as the incident photon energy has been equivalent to the energy variance amid the dual states. Absorbance A is described as the logarithmic relative intensity reduction. As a result, at the supreme absorbance, the wavelength can be indicated as peak wavelength (nm), whereas the extreme absorbance is termed as peak absorbance (arb.unit). The absorption width for the curve at the half magnitude of extreme absorbance can be designated as $(\Delta\nu)_{1/2}$(sec^{-1}) that is considered by the absorption spectrum [13].

2.2. Linear Optical Features

The linear optical features are associated with linear optical response. The absorbance (A) defines the absorbed photons quantity by molecules as shown (1) [14]:

$$A = 1 - \log\left(\frac{1}{T}\right) \quad (1)$$

where T stands for a medium transmittance that is associated with refractive index n as [15-17]:

$$T = \frac{2n}{n^2+1} \quad (2)$$

the coefficient of absorption α of an optical medium is associated with A absorbance in relation to (3) [15-16]:

$$\alpha = \frac{1}{2.302\ A} \quad (3)$$

the effective length L_{eff} of the optical media is computed by [15–17]:

$$L_{eff} = \frac{(1-exp^{-\alpha L})}{\alpha} \quad (4)$$

here, L stands for the sample length and α represents the absorption coefficient.

2.3. Non-linear Optical Features

Several materials suffer from the nonlinear properties as in Kerr nonlinearity that alters the refractive index of a material based on realistic electric field. Z-scan method can be employed to calculate a non-linear absorption coefficient and non-linear refractive index by open and closed apertures, correspondingly. The form of closed aperture supports in determination of minor deformations in generated beam in non-linear media that acts as a miniature non-linear lens and in determining non-linear refractive index as presented in Figure 1 (a). This figure shows an illustration of the closed aperture along with potential recorded data of normalized transmittance.

Open–aperture Z-scan can be employed for determining coefficient of non-linear absorption since the entire laser beam can be incident on the detector with neglected minor deformations. Figure 1 (b) clarifies the structure of Z-scan with open aperture with an illustration of potential records of normalized transmittance. Several changes should be considered in an investigation of non-linear coefficients. For instance, non-linear response of the medium as a result of the laser beam in restricted region as in laser spot area in the media can be influenced as a result of laser beam intensity in the neighbouring regions. This influence is termed as non local response. Another influence acts in the liquid testers of colloid non-linear medium in a dielectric solution. The incident photonic field in non-local medium locations stirs up numerous variations as in molecular dipoles reorientation as a result of the alterations in electric fields in diverse portions of the non-linear media [17].

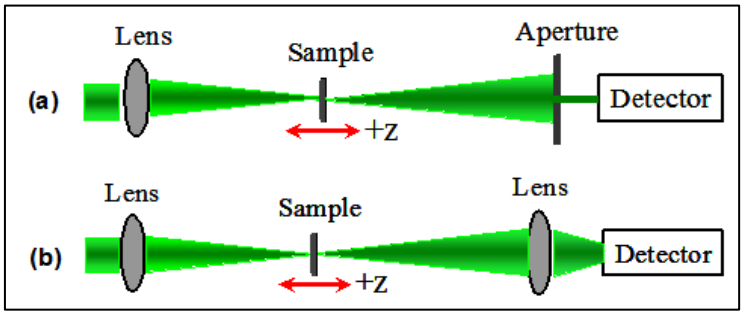

Figure 1. Structure of Z-scan with dual dissimilar schemes and an illustration of potential determined data of normalized transmittance via, (a) closed aperture, (b) open aperture [17]

The non-linear refractive index is feasibly determined by [17-19]:

$$n_2 = \frac{\Delta\Phi_o}{I_o L_{eff} K} \quad (5)$$

where I_o stands for the incident laser intensity, K represents the wavenumber of incident laser beam that is equivalent to $K = \frac{2\pi}{\lambda}$. λ stands for incident laser beam wavelength, whereas $\Delta\Phi_o$ stands for nonlinear phase shift [17-21].

$$\Delta T_{p-v} = 0.406 \left|\Delta\Phi_o\right| \quad (6)$$

In (6), ΔT_{p-v} stands for the normalized transmittance variance amid the topmost and the valley transmittance magnitudes that computed by means of setup of closed aperture Z-scan. The nonlinear absorption parameter β is computed by [20-25]:

$$\beta = \frac{2\sqrt{2}T(Z)}{I_o L_{eff}} \quad (7)$$

$T(Z)$ signifies for the smallest normalized transmittance gotten by setup of open aperture Z-scan.

3. Experiment

About 10^{-3} mol/l molar concentration of IR5 laser dye has organized by (0.001 gm) weighting employing HR-200 digital balance for laser dye. This has dissolved in 10 ml of dichloroethane. About 0.04 gm of PP polymer has inserted to the dye solution. The 0.02 gm of (CdSe) nanoparticles has weighted by means of the similar balance and inserted to the dye mixtures. HP-3000 magnetic stirrer has used to achieve a homogeneous solution. It has used drop-casting way to achieve uniform thin films with five different films thickness as (2, 4, 6, 8 and 10) mm. The prepared thin films of (4 mm) thickness had been irradiated by five different Yb:$GdVO_4$ laser pulses as (25,50,75,100 and 150) $\frac{pulse}{min}$. The absorption spectrums for all the prepared thin films samples were taken by means of Mega -2100 UV-Vis spectrophotometer. The used Z-scan set up has SHG–Nd:YAG laser at 532 nm of green light as a laser source and dedicated for the tester by means of lens of 15 cm focal length. The radius of laser spot has been 0.05 cm, while the incident laser intensity on the tester has been 778 Watt/m^2. The normalized transmittance is feasibly determined by means of LP1-mobiken laser power meter.The normalized transmittance data for organized thin film testers of 4 cm length, controlled by ($3x10^{-3}$ mol/l of (IR5) laser dye, 0.02 gm of (CdSe) nanoparticles and 0.04 gm of pp polymer, were determined by Z-Scan setup of closed and open apertures using LP1-mobiken laser power meter.

4. Results

According to the absorption spectrums taken for the prepared thin films, the linear optical features of that films had been calculated depending on (1, 2, 3, and 4), respectively at different thin films thickness and recorded in Table 1. The effective length was of (0.0494 m) for all the studied samples. Table 2 shows the Linear optical parameters at different Yb:$GdVO_4$ laser pulses. More graphical details are clarified Figures 2 to 3.

Table 1. The Linear Optical Factors of (10^{-3} IR5 Laser Dye, 0.1 gm PP and CdSe Nanoparticles) at Dissimilar thin Films Thicknesses

Thickness mm	A	T	α (m^{-1})	n
2	0.87	0.134	0.499	14.858
4	0.89	0.128	0.488	15.560
6	0.91	0.123	0.477	16.198
8	0.93	0.117	0.467	17.035
10	0.95	0.112	0.457	17.800

Table 2. The Linear Optical Factors of (10^{-3} IR5 Laser Dye, 0.1 gm PP and 0.04 gm of CdSe Nanoparticles) at Dissimilar Yb:GdVO4 Laser Pulses

NO.of Yb:$GdVO_4$ laser pulses	A	T	α (m^{-1})	n
25	0.95	0.112	0.457	17.800
50	0.92	0.120	0.472	16.606
75	0.89	0.128	0.488	15.560
100	0.86	0.138	0.505	14.423
150	0.84	0.144	0.517	13.816

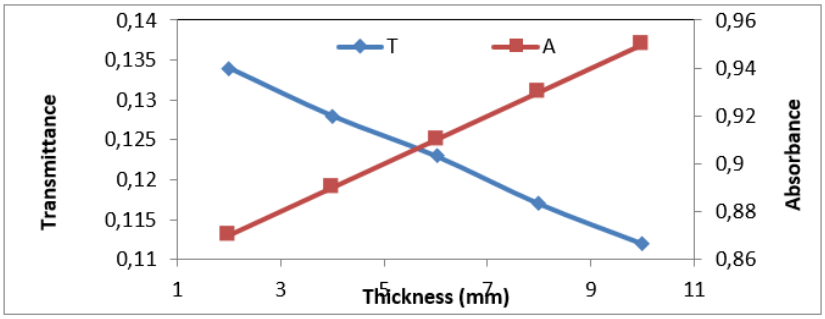

Figure 2. The Linear transmittance and absorbance of (10^{-3} IR5 laser dye, 0.1 gm PP polymer and 0.04 gm of CdSe nanoparticles) at different thin films thickness

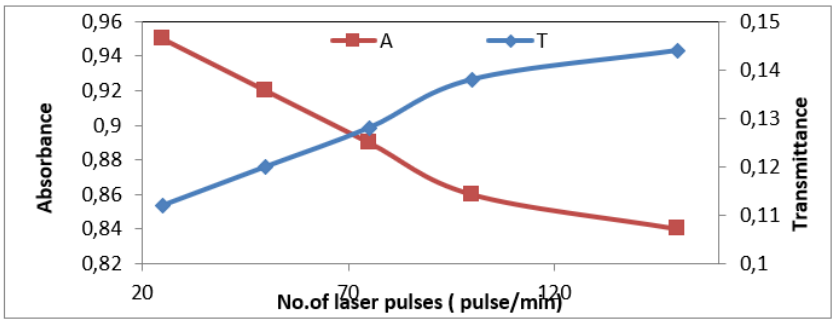

Figure 3. The Linear transmittance and absorbance of (10^{-3} IR5 laser dye, 0.1 gm PP polymer and 0.04 gm of CdSe nanoparticles) at different Yb:GdVO4 laser pulses

Non-linear optical factors such as ΔT_{p-v}, $\Delta\Phi_o$, non-linear refractive index (n_2), $T(Z)$ and β for thin film samples of 10^{-3} IR5 laser dye, 0.1 gm PP polymer and 0.04 gm of CdSe nanoparticles, were determined in relation to the determined data of normalized transmittance by means of Z-Scan of closed and open apertures as illustrated in Figures 4 until 7 and (5, 6 and 7) of non-linear optical features stated in the previous section. These coefficients at different films thickness had been depicted in Table 3, while Table 4 illustrates non-linear optical coefficients at different Yb:$GdVO_4$ laser pulses.

Table 3. The Non-Linear Optical Factors of 10^{-3} IR5 Laser Dye, 0.1 gm PP and 0.04 gm of CdSe Nanoparticles) at Different thin Films Thickness

Thickness mm	ΔT_{p-v}	$\Delta\Phi_o$	n_2 x10^{-9}	$T(Z)$	β x10^{-3} (W^{-1}.m)
2	0.73	1.798	3.969	0.54	39.740
4	0.70	1.724	3.805	0.52	38.268
6	0.67	1.650	3.642	0.49	36.060
8	0.63	1.551	3.423	0.46	33.853
10	0.61	1.502	3.315	0.41	30.173

Table 4. The Non-Linear Optical Factors of (10^{-3} IR5 Laser Dye, 0.1 gm PP and 0.04 gm of CdSe Nanoparticles) at Different Yb:$GdVO_4$ Laser Pulses

No.of Yb:$GdVO_4$ laser pulses	ΔT_{p-v}	$\Delta\Phi_o$	n_2 x10^{-9}	$T(Z)$	β x10^{-3} (W^{-1}.m)
25	0.68	1.674	3.695	0.44	32.381
50	0.7	1.724	3.805	0.47	34.589
75	0.74	1.822	4.022	0.50	36.794
100	0.78	1.921	4.240	0.53	39.004
150	0.81	1.995	4.403	0.55	40.476

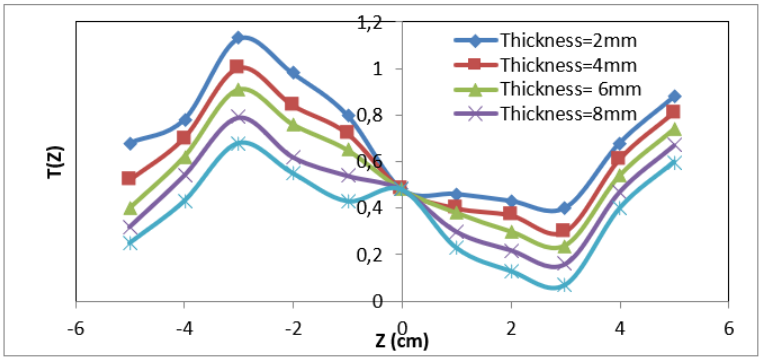

Figure 4. The normalized transmittance of (10^{-3} IR5 laser dye, 0.1 gm PP polymer and 0.04 gm of CdSe nanoparticles) at different thin films thickness, using closed aperture Z-scan setup

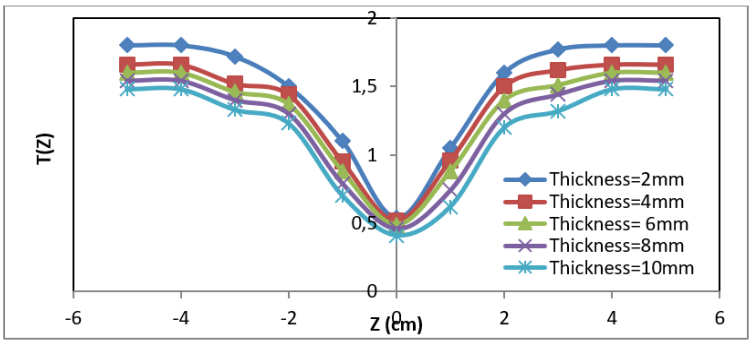

Figure 5. The normalized transmittance of (10^{-3} IR5 laser dye, 0.1 gm PP polymer and 0.04 gm of CdSe nanoparticles) at different thin films thickness, using open aperture Z-scan setup

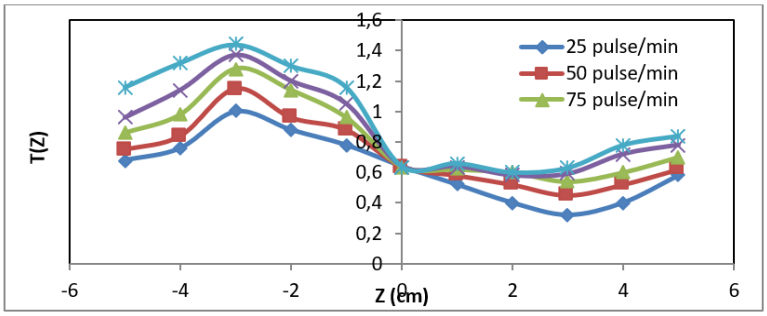

Figure 6. The normalized transmittance of (10^{-3} IR5 laser dye, 0.1 gm PP polymer and 0.04 gm of CdSe nanoparticles) at different Yb:GdVO4 laser pulses, using closed aperture Z-scan setup

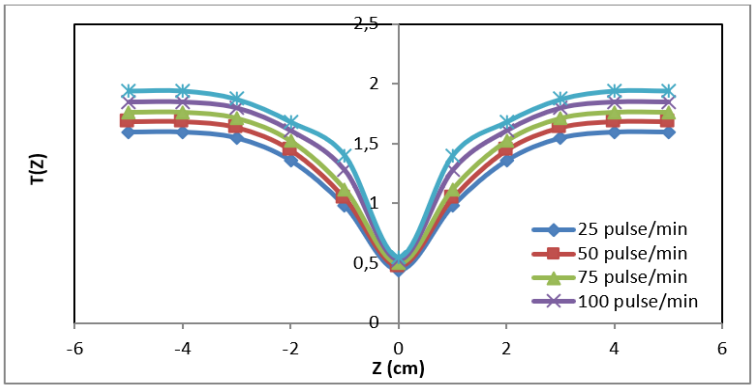

Figure 7. The normalized transmittance of (10^{-3} IR5 laser dye, 0.1 gm PP polymer and 0.04 gm of CdSe nanoparticles) at different Yb:GdVO4 laser pulses, using open aperture Z-scan setup

5. Discussion

Table 1 shows the linear optical features (A , T , α and n) intended for thin film samples of (10^{-3} IR5 laser dye , 0.1 gm PP and CdSe nanoparticles) at dissimilar thin films thickness as (2, 4, 6, 8 and 10) mm. Figure 2 illustrates the (T and A) behaviour for thin film thickness. The increase in thin film thickness causes an increasing for both of (A and n) and decreasing for both of (T and α). This due to that the highest thickness consolidates the absorption process because of the highest molecules in the ground state (g.s) which able to absorb more energy than that of less film thickness. This leads to highest transmittance for incident light energy. Because of highest absorption probability for highest media thickness, this medium becomes more refractive than air and possess less absorption coefficient.

Figures 4 and 5 show the normalized transmittance for thin films of (10^{-3} IR5 laser dye, 0.1 gm PP as well as CdSe nanoparticles) at diverse thin films thickness using closed and open aperture Z-scan setup, respectively. It is obvious that the increasing of films thickness reduces both of the difference between top–transmittance point and valley-transmittance point $\Delta \boldsymbol{T_{p-v}}$ in the closed-aperture curve, and the minimum transmittance in the open-aperture curve $\boldsymbol{T(Z)}$. This can be attributed to the highest scattering due to larger thickness, which reduces the ($\Delta \boldsymbol{T_{p-v}}$ and $\boldsymbol{T(Z)}$) for both of closed-aperture and open-aperture normalized transmittance curves.

Table 3 illustrates the non-linear optical coefficients as ($\Delta \boldsymbol{T_{p-v}}$, $\boldsymbol{T(Z)}$,$\Delta \boldsymbol{\Phi_o}$, $\boldsymbol{n_2}$ and $\boldsymbol{\beta}$) at different thin films thickness. Where all of the described non-linear coefficients are decreased with the increasing of thin films thickness. This behaviour can be interpreted depending on medium transmittance decreasing for thick medium which consolidates the non-linear effects inside the sample.

By changing the amount of incident Yb:GdVO4 laser pulses on the sample, the linear and non-linear optical features of the studied sample, had been changed. Figure 3 shows the (T and A) behaviour as a function of No. of laser pulses and Table 2 illustrates the linear optical features at different laser pulses. It is clear that the highest laser pulses number causes an increasing in both of (T and α) and a decreasing in both of (A and n). The highest number of incident laser pulses contributes in exciting more ground-state molecules to higher excited states, so no more molecules found in ground state, which makes the absorption process is weak vice inverse for transmittance which becomes strong.

The effect of incident laser pulses in the non-linear optical features has recorded in Table 4 and depicted for closed-aperture and open-aperture in Figures 6 and 7, respectively. The strongest non-linear features which appears when more laser pulses are used, can be attributed to highest electric field generated inside the sample irradiated by more laser pulses. This induces more induction polarization causeing an increase in non-linear refractive index, absorption coefficient and phase shift.

6. Conclusion

It can be concluded that the sample of (10 mm) thickness has less non-linear optical features than other studied samples. The same sample has highest (A and n) and less (T and α) linear optical features. The $150\ \frac{pulse}{min}$ of Yb:$GdVO_4$ causes highest non-linear optical features and (T and α) linear optical features; while it is the main reason to reduce both of (A and n) linear optical features. The most important outcome is that the thick films cause deleting the non-linear effects generated by different layers. While, the highest amount of laser pulses consolidates the non-linear effects as the highest electric field generated through film irradiated by laser.

References

[1] Yang H, Liu W, Xu C, Fan D, Cao Y, Xue W. Laser Sintering of TiO2 Films for Flexible Dye-Sensitized Solar Cells. *Applied Sciences*. 2019; 9(5): 823.
[2] Alfano R, Schiller N, Reynolds G. Production of picosecond pulses by mode locking an Nd: glass laser with dye#5. *IEEE Journal of Quantum Electronics*. 1981; 17(3): 290-291.
[3] Lifshitz E, Dag I, Litvin I, Hodes G, Gorer S, Reisfeld R, Zelner M, Minti H. Optical properties of CdSe nanoparticle films prepared by chemical deposition and sol–gel methods. *Chemical Physics Letters*. 1998; 288(2-4):188-196.
[4] Zhang S, Yu J, Li X, Tian W. Photoluminescence properties of mercaptocarboxylic acid-stabilized CdSe nanoparticles covered with polyelectrolyte. *Nanotechnology*. 2004; 15(8): 1108-1112.
[5] Sondi I, Siiman O, Matijevic E. Synthesis of CdSe nanoparticles in the presence of aminodextran as stabilizing and capping agent. *J. Colloid Interface Sci*. 2004; 275: 503-507.
[6] Boatman EM, Lisensky GC, Nordell KJ. A safer, easier and faster synthesis for CdSe quantum dots nanocrystals. *J. Chem. Educ.* 2005; 82(11) :1697.
[7] Gupta P, Ramrakhiani M. Influence of the Particle Size on the Optical Properties of CdSe Nanoparticles. *The Open Nanoscience Journal*. 2009; 3: 15-19.
[8] Whiteley SK, Heggs TG, Koch H, Mawer RL, Polyolefins WI. Encyclopedia of Industrial Chemistry. Weinheim: Wiley-VCH. 2005.
[9] Stinson S. Discoverers of Polypropylene Share Prize. *Chemical & Engineering News*. 1987; 65(10): 30.
[10] Morris PJ. Polymer pioneers: a popular history of the science and technology of large molecules. Chemical Heritage Foundation. 2005; 5: 76.
[11] Kaiser W. Kunststoffchemie für Ingenieure: von der Synthese bis zur Anwendung. Carl Hanser Verlag GmbH Co KG. 2015.
[12] Iakovlev VV, Guelcher SA, Bendavid R. Degradation of polypropylene in vivo: a microscopic analysis of meshes explanted from patients. *Journal of Biomedical Materials Research Part B: Applied Biomaterials*. 2017; 105(2): 237-248.
[13] Elmer P. An introduction to fluorescence spectroscopy. HP9 1QA, printed in UK, Perkinelmer, Inc. 2000: 16-17.
[14] Nicholas M. Electromagnetic spectrum: transmittance, absorbance and reflectance. *RST technical and historical perspectives of remote sensing*. 2007: 1-5.
[15] Abdul-Wahid SN, Al- Sultani MMM. Study of the optical properties for BDN-I dye solutions which are used to Q-switch the Nd:YAG laser. *Journal of Kerbala University*. 2008; 6(1): 33-54.

[16] Kim GY, Kwak CH. Simple Optical Methods for Measuring Optical Nonlinearities and Rotational Viscosity in Nematic Liquid Crystals. In New Developments in Liquid Crystals-Intech Open. Vienna. 2009.
[17] Ara MM, Dehghani Z, Sahraei R, Nabiyouni G. Non-linear optical properties of silver nanoparticles prepared by hydrogen reduction method. *Optics Communications*. 2010; 283(8): 1650-1653.
[18] Mahdi ZF, Ali AA. Investigation of nonlinear optical properties for laser dyes-doped polymer thin film. *Iraqi Journal of Physics*. 2012; 10(19): 54-69.
[19] Ao G, Xiao Z, Qian X, Li Z, Wang Y, Zhang X, Song Y. Nonlinear optical properties tuning in meso-tetraphenylporphyrin derivatives substituted with donor/acceptor groups in picosecond and nanosecond regimes. *Molecules*. 2015; 20(4): 5554-5565.
[20] Ganeev RA, Baba M, Ryasnyansky AI, Suzuki M, Kuroda H. Characterization of optical and nonlinear optical properties of silver nanoparticles prepared by laser ablation in various liquids. *Optics Communications*. 2004; 240(4-6): 437-448.
[21] Marble CB, Clary JE, Noojin GD, O'Connor SP, Nodurft DT, Wharmby AW, Rockwell BA, Scully MO, Yakovlev VV. *Nonlinear optical properties of water from 1150 nm to 1400 nm*. In Optical Interactions with Tissue and Cells XXX 2019 Mar 1. International Society for Optics and Photonics. 2019; 10876: 108760I.
[22] Jassim MJ, Khadim YH, Al-Sultani MMM. Study the effect of the particle size of the scattering centers in each of a linear and non-linear optical property for the laser random media. *Journal of Engineering and Sciences*. 2018; 13(1): 80-88.
[23] Jassim JM, Khadim YH, Al-Sultani MMM. Study of linear and non-linear optical properties for the thin films of laser dye–Fe_3O_4 nano particles doped PMMA thin films. *Journal of Engineering and Applied Sciences.* 2018; 13(22): 9511-9518.
[24] Nozaki K, Matsuo S, Fujii T, Takeda K, Shinya A, Kuramochi E, Notomi M. Femtofarad optoelectronic integration demonstrating energy-saving signal conversion and nonlinear functions. *Nature Photonics*. 2019: 1.
[25] Namarathne DL, Walden SL, Donaldson RE, Jaatinen EA. Using Image Analysis to Determine Ideal Aperture Conditions for Optimal Z-Scan Signal Quality. *IEEE Journal of Quantum Electronics*. 2018; 54(3): 1-9.